PAPER

Check for updates

Reorientation of π-conjugated molecules on few-layer MoS₂ films†

Jakub Hagara, [ID] [a] Nada Mrkyvkova, [ID] *[ab] Peter Nádaždy,[a] Martin Hodas, [ID] [c]
Michal Bodík, [ID] [a] Matej Jergel, [ID] [ab] Eva Majková, [ID] [ab] Kamil Tokár, [ID] [ad]
Peter Hutár,[e] Michaela Sojková, [ID] [e] Andrei Chumakov, [ID] [f] Oleg Konovalov,[f]
Pallavi Pandit,[g] Stephan Roth,[g] Alexander Hinderhofer,[c] Martin Hulman, [ID] [e]
Peter Siffalovic [ID] [ab] and Frank Schreiber [ID] [c]

Small π-conjugated organic molecules have attracted substantial attention in the past decade as they are considered as candidates for future organic-based (opto-)electronic applications. The molecular arrangement in the organic layer is one of the crucial parameters that determine the efficiency of a given device. The desired orientation of the molecules is achieved by a proper choice of the underlying substrate and growth conditions. Typically, one underlying material supports only one inherent molecular orientation at its interface. Here, we report on two different orientations of diindenoperylene (DIP) molecules on the same underlayer, *i.e.* on a few-layer MoS₂ substrate. We show that DIP molecules adopt a lying-down orientation when deposited on few-layer MoS₂ with horizontally oriented layers. In contrast, for vertically aligned MoS₂ layers, DIP molecules are arranged in a standing-up manner. Employing *in situ* and real-time grazing-incidence wide-angle X-ray scattering (GIWAXS), we monitored the stress evolution within the thin DIP layer from the early stages of the growth, revealing different substrate-induced phases for the two molecular orientations. Our study opens up new possibilities for the next-generation of flexible electronics, which might benefit from the combination of MoS₂ layers with unique optical and electronic properties and an extensive reservoir of small organic molecules.

[a] *Institute of Physics, Slovak Academy of Sciences, Dúbravská Cesta 9, 845 11 Bratislava, Slovakia. E-mail: nada.mrkyvkova@savba.sk*

[b] *Center for Advanced Materials Application, Slovak Academy of Sciences, Dúbravská Cesta 9, Bratislava 84511, Slovakia*

[c] *Institute of Applied Physics, University of Tübingen, Auf der Morgenstelle 10, D-72076 Tübingen, Germany*

[d] *Advanced Technologies Research Institute, Faculty of Materials Science and Technology in Trnava, Slovak University of Technology in Bratislava, 917 24 Trnava, Slovakia*

[e] *Institute of Electrical Engineering, Slovak Academy of Sciences, Dúbravská Cesta 9, 845 11 Bratislava, Slovakia*

[f] *European Synchrotron Radiation Facility, 71 Avenue des Martyrs, Grenoble 38000, France*

[g] *Photon Science, Deutsches Elektronen-Synchrotron (DESY), Hamburg 22607, Germany*

† Electronic supplementary information (ESI) available: Orientation of π-conjugated molecules controlled by few-layer MoS₂ films. See DOI: 10.1039/c9cp05728e

Small organic semiconductors based on π-conjugated molecules attracted considerable attention in the past decade,[1] due to their prospective applications in the area of flexible electronics. Since most of the π-bonded molecules are anisotropic in shape, the electrical and optical properties of organic thin films strongly depend on molecular orientations with respect to the underlying substrate. This means that the efficiency of a specific application is directly determined by the molecular orientations.[2–5] For example, for rod-like molecules with the transition dipole moment along the long axis, the lying-down orientation is beneficial in organic photovoltaics to optimize optical absorption and electric transport.[2,4] On the other hand, the standing-up orientation of molecules is usually favorable for (in-plane) organic field-effect transistors (OFETs), where the maximum charge-carrier mobility is observed in the direction of π-stacking.[1,6,7] Generally, the required molecular alignment is achieved by selecting appropriate growth conditions and/or substrates.[2–4,8–12] The standing-up orientation is typically achieved on oxides, as in the case of the insulation layers of many OFETs, where the van der Waals interactions among the molecules are stronger than the molecule–substrate interactions.[3,9,13] The lying-down order is adopted on strongly interacting substrates such as metals and semiconductors,[9,14,15] or on two-dimensional (2D) layers where the interactions between the molecules and substrates are comparable or stronger.[11,16] We note that this classification is not universal, as other factors concerning cleanliness and symmetry might affect the growth direction as well.[10,12,17,18]

In this study, we report on orientational control of diindeno-perylene (DIP),[19–22] one of the representatives of rod-like π-conjugated molecules, by choice of few-layer MoS_2 substrates. Few-layer MoS_2 belongs to a group of two-dimensional (2D) transition metal dichalcogenides (TMDCs), which are receiving attention due to their remarkable properties compared with their bulk counterparts.[23–25] TMDCs show a unique combination of atomic-scale thickness, direct bandgap in the NIR-VIS range in the case of a monolayer and advantageous electronic properties, which not only make them interesting for fundamental studies, but also for applications in optoelectronics, spintronics, flexible electronics, energy harvesting, sensors *etc.*[23,26–28] The recent advances in sample preparation (mainly driven by graphene research) enabled fabrication and characterization of TMDCs, where MoS_2 layers belong to the most widely studied ones. There are several growth techniques for few-layer MoS_2 films,[29] predominantly leading to horizontally aligned atomic planes, *i.e.* MoS_2 layers aligned parallel to the substrate plane. This surface termination shows minimal roughness with no dangling bonds, which is ideal for electronic devices and applications.[23,30] Recently, attention has also been paid to vertically aligned MoS_2 layers. In the vertical configuration, the MoS_2 layers are aligned perpendicular to the substrate, exposing the edge sites. As the edges contain dangling bonds, the vertical alignment of MoS_2 finds its application in various catalytic reactions, *e.g.* hydrogen evolution electrocatalysis[31] or water disinfection.[32]

In this work, we utilized few-layer MoS_2 with both orientations of the atomic layers as the underlying substrate for manipulating the molecular orientations. The MoS_2 layers were prepared by the so-called one-zone sulfurization technique.[33] It has been found that the conditions under which sulfurization takes place can be employed to control the resulting MoS_2 orientation, enabling the preparation of both orientations either by changing the thickness of the Mo base-layer[34] or the rate of the sulfur heating. We show that the orientation of MoS_2 layers directly influences the orientation of small organic molecules and thus the overall physical properties, *e.g.* optical absorption. These observations are of particular interest as they show the ability to orient the rod-like molecules either in the lying-down or standing-up orientation on a single, electronically relevant templating material, under the same conditions of molecular growth. This phenomenon might find its application in future (opto-)electronic flexible devices where the marriage of TMDCs and organics could benefit from the advantageous properties of both semiconducting materials.[35,36]

Results and discussion

The thin MoS_2 layers used in this work were produced by the rapid sulfurization growth technique[29,33,34,37] of Mo films. This technique enables the fabrication of large-area MoS_2 crystalline layers of high quality. Sulfurization of 1 and 3 nm thick Mo films rulted in MoS_2 layers with a thickness of 3 and 9 nm, respectively. Interestingly, the same growth conditions lead to a different alignment of MoS_2 atomic layers in these samples. The orientation of MoS_2 layers was determined by grazing-incidence wide-angle X-ray scattering (GIWAXS), where the 002 diffraction with a q-vector magnitude of ~ 1 Å^{-1} was clearly visible – see Fig. 1. The scheme of the GIWAXS setup can be found in the ESI,† see Fig. S1. For the 3 nm thick MoS_2 layer, the crystallographic c-axis points along q_z, *i.e.* parallel to the substrate normal n (inset in Fig. 1a), indicating the horizontal orientation of the MoS_2 atomic layers. On the other hand, for the 9 nm thick MoS_2 layer the c-axis is perpendicular to the substrate normal (inset in Fig. 1b), which implies the vertical alignment of the layers. A weak 002 diffraction under the "missing wedge"[38,39] at 1 Å^{-1} suggests the presence of horizontally oriented MoS_2 grains. However, their ratio to the vertically aligned MoS_2 layers is marginal.

The orientation of the MoS_2 layers subsequently influences the orientation of DIP molecules. Fig. 1 shows the 001 diffraction peak positions of DIP layers (Bragg reflection at $q \approx 0.39$ Å^{-1}) grown on 3 and 9 nm thick MoS_2 films. On the horizontally aligned MoS_2, we also detected the $\bar{1}10$ diffraction peak ($q \approx 1.15$ Å^{-1}), see Fig. 1a. More diffraction spots were observed
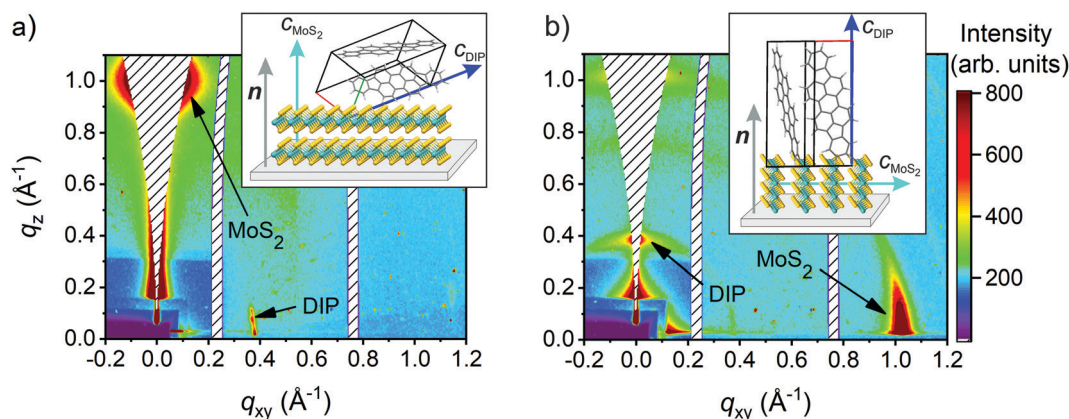
Fig. 1 Reciprocal space map measured in the GIWAXS geometry for a 12 nm thick DIP film grown on (a) 3 nm and (b) 9 nm MoS_2 layers. Both patterns show the 001 Bragg reflection of DIP ($q \approx 0.39$ Å^{-1}) and the 002 Bragg reflection of MoS_2 ($q \approx 1$ Å^{-1}). The mutual orientations of the c-axes of DIP and MoS_2 are schematically shown in the insets.

3098 | *Phys. Chem. Chem. Phys.*, 2020, **22**, 3097–3104

This journal is © the Owner Societies 2020

for DIP thin films on a MoS_2 monolayer, which were used to calculate the full set of unit cell parameters and the molecular orientation within the unit cell.[40] For few-layer MoS_2 substrates this was not possible because of the reduced intensity in diffraction peaks other than 001. The detected diffractions yield only the information about the unit cell orientation with respect to the surface. In order to determine the molecular orientation, one needs to know their position within the crystallographic unit cell. Taking advantage of the recently calculated orientation of the DIP molecules within the unit cell on MoS_2 monolayers,[40] we can conclude that the molecules adopt the "lying-down" configuration on the horizontally aligned MoS_2. In contrast, for the vertically aligned MoS_2 films, the DIP molecules are organized in the "standing-up" manner. We note that this feature is not limited only to DIP molecules, but it has more general validity and applies to other π-conjugated systems as well. We observed the same character of molecular alignment also for pentacene and 5,5′-bis(naphth-2-yl)-2,2′-bithiophene (NaT2) – more information about NaT2 molecules can be found in ref. 41.

Furthermore, we would like to emphasize that the molecular orientation is influenced solely by the orientation of the underlying atomic layers and not by the layer thickness. We observed the lying-down orientation of DIP molecules also for 9 nm thick MoS_2 layers, where the specific conditions of the sulfurization enabled the horizontal alignment of the atomic layers.[42] The orientation of the molecules is thus given by the molecular interaction with the underlying substrate. Both types of our MoS_2 substrates show similar surface roughness (in the order of a few nanometers), but different surface energy – being higher for the vertically aligned MoS_2.[28] This agrees well with the assumption that the vertical layers exhibit more dangling bonds which are chemically active[37] and readily oxidized. Consequently, such an oxidized surface exhibits a weaker interaction with the deposited molecules. On the other hand, the absence of dangling bonds in the horizontally aligned MoS_2 layers causes the molecule–substrate interaction being comparable with the molecule–molecule interaction, which leads to the in-plane molecular orientation.

In Fig. 1, a vertically doubled 001 diffraction peak can be seen, which is caused by the substrate-induced total reflection at small incidence angles.[43] This multiple scattering effect is well described by the distorted wave Born approximation[44] and it is more pronounced in Fig. 1a. The lower peak of the diffraction doublet represents a direct scattering channel within the DIP layer. The upper peak arises as a combination of two effects – the total reflection of the incoming X-ray beam at the substrate/organic interface and the subsequent Bragg diffraction in the organic film.[43] The duplicity of the 001 diffraction is hardly visible for the "standing-up" molecules in Fig. 1b, because it is partially shadowed by the "missing wedge", which arises in the grazing-incidence geometry. Apart from the above mentioned multiple scattering effect, an enhanced diffracted intensity at the critical exit angle is visible at $q_z \approx 0.03$ Å^{-1} (exit angle $\alpha_f \approx 0.18°$). In general, α_f coincides with the critical angle of the scattering material. However, in

this case, it corresponds to the average of the critical angles for DIP and MoS_2 as both layers contribute to the scattering.[43,45]

Furthermore, we studied the time-evolution of the two molecular orientations of DIP on MoS_2 during the growth. We performed *in situ* and real-time GIWAXS measurements in order to track the 001 diffraction positions for both samples. The 001 diffraction position is related to the orientation and magnitude of the unit cell vector *c*. The thickness dependence of the *c* parameter is shown in Fig. 2 for both molecular orientations. The early stages of DIP growth were measured at a synchrotron facility, where the intensity of the X-ray beam is sufficient for the detection of even a few molecular layers. The time-consuming measurements of the thicker layers were performed in the laboratory. Unfortunately, the intensity of the beam under the laboratory conditions does not allow for a precise determination of the *c*-parameter for layers thinner than 10 nm. We would like to note that we use the term effective thickness throughout the whole manuscript to define the thickness of the grown layers with standing-up and lying-down molecules. The effective thickness indicates the laterally averaged thickness of the DIP layer grown on the silicon substrate in the layer-plus-island (Stranski–Krastanov) growth mode.[3,13,22] In this mode, the molecular layers can be well distinguished, and one can reliably measure their thickness.

Fig. 2 shows a similar evolution of the unit cell *c*-parameter for both orientations of the DIP molecules. The *c*-parameter continuously increases with the effective layer thickness up to 12 nm and saturates afterward. Clearly, the saturated value of *c* is different for the two molecular orientations and neither of them coincides with the *c*-parameter measured in the bulk crystal.[20] This indicates that we observe a heavily strained or distorted structure, which may be considered a different bulk polymorph. The bulk-phase polymorphism was recently found also for pentacene,[46] which is perceived as a model molecule for organic film growth studies. For pentacene, different scenarios
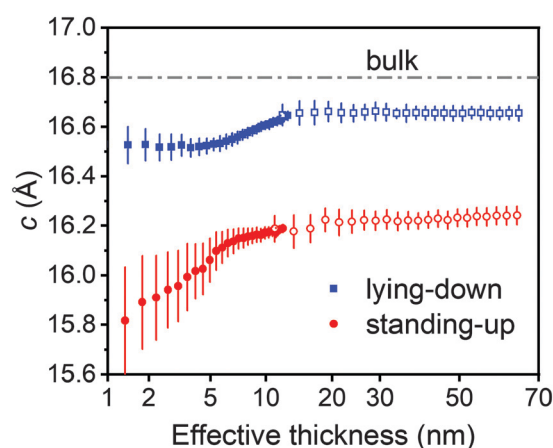

Fig. 2 The lattice parameter *c* for the lying-down (blue) and standing-up (red) orientations of DIP molecules as a function of the effective layer thickness. The solid points represent the data measured under the synchrotron conditions while the open points stand for the data measured under the laboratory conditions. The dashed grey line indicates the *c*-parameter of the bulk DIP crystal (taken from ref. 20).

This journal is © the Owner Societies 2020

Phys. Chem. Chem. Phys., 2020, **22**, 3097–3104 | **3099**

of the thin-film to bulk phase transition were reported previously, *e.g.* the independent nucleation and growth of the two phases[47] or the occurrence of the bulk phase at the critical thickness of the thin-film phase.[48,49] In our case, we observe a continuous transition between the thin-film and bulk phases, which is intrinsic to the inorganic heteroepitaxial systems, typically.[50] The continuous variation of the *c*-parameter can be explained by a gradual relaxation of the strain induced by the lattice mismatch between the DIP layer and the substrate. The *c*-parameter increase might indicate a gradual deflection of the molecules with respect to the underlying substrate, *i.e.* reducing (enlarging) the angle between the molecules and the MoS_2 layer for the lying-down (standing-up) molecular orientation. An alternative explanation of the *c*-parameter increase might be that the molecules in the unit cell are shifting away, each of them in the opposite direction of the *c*-axis. In order to identify the actual case, further measurements supported by additional calculations would be needed.[40]

Now, we would like to focus on the morphology of the grown molecules on the few-layer MoS_2 surface. It is known that the standing-up and lying-down molecular orientations show distinct growth modes,[22,40,51,52] which we also confirmed by AFM. Fig. 3 shows AFM images of DIP layers with different orientations of molecules, which were grown on vertically [(a), (b), (c) and (d)] and horizontally [(e), (f), (g) and (h)] aligned MoS_2 layers. The scans were performed at several random positions of the sample surface and the scanning area was $5 \times 5 \ \mu m^2$ for all samples. For vertical MoS_2 layers, the surface is presumably oxidized because of the chemically reactive dangling bonds. In this case, we assume that the molecules grow in the layer-plus-island mode, similarly as on other oxidized surfaces, such as SiO_2 or ITO.[3,22,53] The individual layers are hardly distinguishable on vertically aligned MoS_2 due to the grainy structure of its surface, see Fig. 3(a)–(d). It is evident that the molecules cover the whole area of the exposed surface. However, if the molecules are deposited on 2D substrates, where the basal planes with a minimum number of dangling bonds are the terminating surface, they will create isolated islands

(Volmer–Weber growth mode).[40,51] Island-type of growth was indeed observed for the 3 nm thick MoS_2 layer, see Fig. 3(e)–(h). Fig. 3 also shows the DIP layers with various effective thicknesses. We observed the expected height increase with the increasing effective thickness for the standing-up molecules [Fig. 3(a)–(d)]. For the needle-like islands in Fig. 3(e)–(h) we observe the same tendency, *i.e.* the height increase dominates the modification in width and length. The average height of the islands is higher when compared with the same effective thickness for the standing-up molecules. This is in accordance with the fact that the same amount of molecules is assembled on a much smaller area (molecules are confined within the islands which have a much smaller overall area than the whole substrate where the standing-up molecules are evenly distributed).

In the following, we will discuss the optical absorption properties of the two molecular orientations. The absorption of the molecular layer is not only important in terms of the efficiency of a potential photo-sensitive device,[2] but it also encodes the geometric structure and confinement of the molecules and thus the electronic and transport properties.[54–56] Fig. 4 shows the absorption spectra measured for different effective thicknesses of DIP layers in lying-down and standing-up orientations of the molecules. The absorption of the DIP layer was obtained by subtracting the absorbance of the bare MoS_2 substrate (before DIP deposition). For the as-measured absorption spectra (with MoS_2 layers) see Fig. S2 in the ESI.† The absorption spectra for the lying-down molecular orientation in Fig. 4 show a typical behavior for a molecular π-system.[54] The spectrum reflects the electron excitation from the highest occupied molecular orbital (HOMO) to the lowest unoccupied molecular orbital (LUMO), where the energy spacing between the individual vibronic progressions is $\Delta E = 0.17 \pm 0.01$ eV.[54,56,57] We note that, strictly speaking, an electron–hole pair is excited, and the absorption energy does not exactly correspond to the HOMO–LUMO gap. Nevertheless, for simplicity we adopt the terminology of a HOMO–LUMO transition. We observed an energy shift of the lowest vibronic subband (E_{00}) of the HOMO–LUMO transition with the
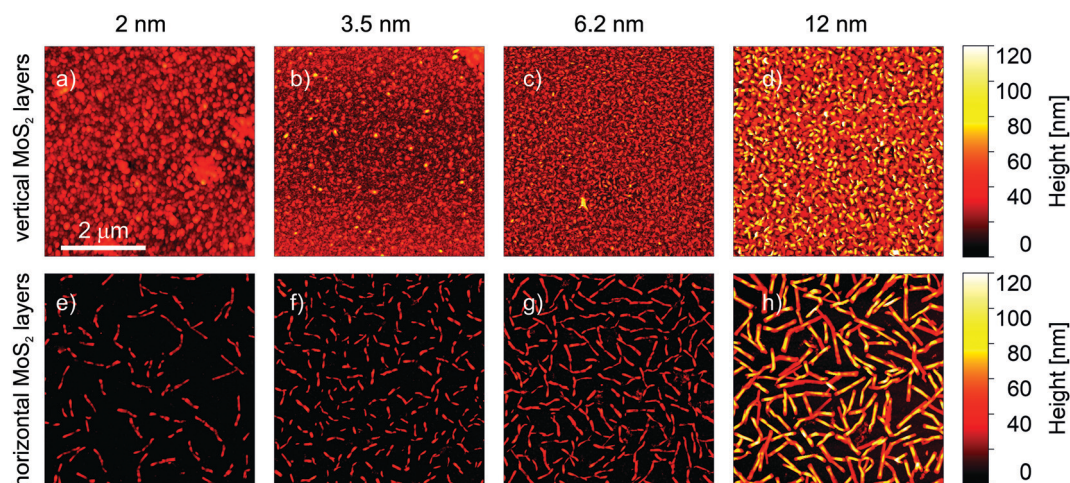

Fig. 3 AFM images of DIP layers grown on vertically (upper row) and horizontally (lower row) aligned MoS_2 layers. The effective thickness of the samples was (from left) 2 nm, 3.5 nm, 6.2 nm and 12 nm.

3100 | *Phys. Chem. Chem. Phys.*, 2020, **22**, 3097–3104

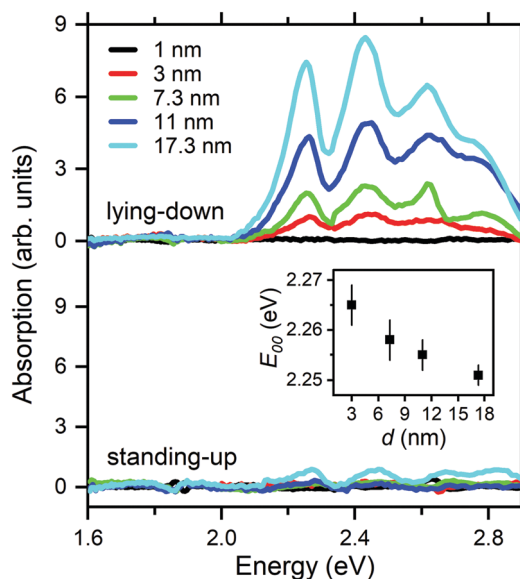This journal is © the Owner Societies 2020

Fig. 4 Optical absorption spectra of DIP layers with different effective thicknesses having lying-down and standing-up molecular orientations. The absorption for lying-down and standing-up molecules is comparable on a relative scale, being ten times larger for the lying-down orientation. The inset shows the energy position of the first absorption peak E_{00} versus the effective film thickness for the lying-down molecular orientation.

increasing DIP thickness, see the inset in Fig. 4. The redshift of E_{00} with the increasing film thickness was also reported by Heinemeyer *et al.* for various π-conjugated molecules.[55] It was attributed to the enhanced dielectric screening caused by increasing molecular coverage.[55,58,59]

Fig. 4 clearly shows a gradual increase of the absorbance with an increasing DIP thickness for the lying-down orientation of the molecules. For the standing-up molecules, no spectral features are visible. This can be explained by a different orientation of the molecular transition dipole moment μ with respect to the incident electric field E. In the studied energy range, μ is aligned parallel to the long molecular axis,[20] causing a minimal projection to E for the standing-up molecules and a maximal projection for the lying-down molecules (in the case of realized normal incidence of light).[2] Accordingly, the absorption cross-section increases with the increasing DIP thickness due to the favorable orientation of the π–π⋆ transition dipole. Similar results were obtained for PTCDA molecules, which typically adopt a lying-down orientation on different substrates as well.[58] Finally, we would like to stress that we also observed a distinct character of the Raman spectra of the thin films with the lying-down and standing-up molecular orientations. A brief discussion of this phenomenon can be found in the ESI.†

Conclusions

In conclusion, we have studied the orientation of DIP molecules on few-layer MoS_2 substrates with a different alignment of the atomic layers. We determined the exact orientation of the molecules employing the GIWAXS technique. We found that for the horizontally aligned MoS_2 layers, DIP adopts a lying-down orientation, whereas the standing-up orientation of DIP is inherent to the vertically stacked MoS_2 layers. Furthermore, AFM measurements revealed distinct growth modes for the two molecular orientations – layer-plus-island mode for the standing-up and island-like (3D) mode for the lying-down molecular orientations. The complementary optical measurements of the absorption spectroscopy showed different spectra of the molecules with respective parallel and perpendicular orientations. The optical data confirmed the importance of the proper molecular orientation in organic-based (opto-)electronic applications (*e.g.* organic solar cells). The *in situ* GIWAXS measurements enabled the determination of the crystallographic *c*-parameter in time, which in turn provides the information about the stress evolution for the two perpendicular molecular orientations. Additionally, we also observed two bulk polymorphs grown on few-layer MoS_2, having a different structure than the bulk crystal obtained by the sublimation technique under streaming gas.[20]

Methods

Few-layer MoS_2 thin films were prepared by magnetron sputtering of 1 nm and 3 nm thick molybdenum layers onto 0001 Al_2O_3 substrates. Mo films were subsequently sulfurized in vapors at 800 °C in the inert atmosphere of N_2.[34] The final thickness of the produced MoS_2 films was 3 nm and 9 nm, respectively. The MoS_2 characterization using the GIWAXS method showed a high degree of film crystallinity and no residual Mo grains.

DIP thin films were prepared in a vacuum chamber by organic molecular beam deposition (OMBD).[60,61] DIP powder was heated up to 255 °C in an effusion cell and evaporated onto the MoS_2 layers, which were annealed prior to the deposition in order to desorb any unfavorable surface contamination. The temperature of the substrates was kept constant at 50 °C during the whole deposition. The pressure was below 2×10^{-8} mbar and the average deposition rate was ~ 1.5 Å min^{-1} (monitored in real time with a quartz crystal microbalance).[40] The GIWAXS measurements were performed at ESRF (Grenoble, France) on the ID10 beamline. The energy of the beam was set to 9.25 keV ($\lambda = 1.34$ Å^{-1}) and the angle of incidence (α_i) was set to 0.2°. The intensity of the X-ray beam was attenuated to 10^{10} photons per s on a spot size of ~ 1 mm^2, which was the highest possible that did not damage the grown molecules on the time-scale of the experiment. The DIP growth was performed in a custom-built chamber outfitted with a 360° cylindrical beryllium window, in order to reduce the scattering of the incident and outgoing beam and to detect the wide-angle diffractions. The detection was done using an area detector Pilatus 300K (Dectris) with a 320 μm thick Si sensor.

The *ex situ* absorbance spectra were measured using a UV-VIS-NIR spectrophotometer Shimadzu SolidSpec-3700. The detected energy range was from 1.6 eV to 2.9 eV with a spectral resolution of 13 meV. The beam spot size at the sample was in the order of a few millimeters, thus probing an average in-plane orientation for

This journal is © the Owner Societies 2020

Phys. Chem. Chem. Phys., 2020, **22**, 3097–3104 | **3101**

the lying-down molecules and the average out-of-plane orientation for the standing-up molecules.

Conflicts of interest

There are no conflicts to declare.

Acknowledgements

References

1 C. D. Dimitrakopoulos and P. R. L. Malenfant, Organic Thin Film Transistors for Large Area Electronics, *Adv. Mater.*, 2002, **14**(2), 99–117, DOI: 10.1002/1521-4095(20020116)14: 2<99::AID-ADMA99>3.0.CO;2-9.

2 C. Schünemann, D. Wynands, K. J. Eichhorn, M. Stamm, K. Leo and M. Riede, Evaluation and control of the orientation of small molecules for strongly absorbing organic thin films, *J. Phys. Chem. C*, 2013, **117**(22), 11600–11609.

3 L. Zhang, S. S. Roy, N. S. Safron, M. J. Shearer, R. M. Jacobberger and V. Saraswat, *et al.*, Orientation Control of Selected Organic Semiconductor Crystals Achieved by Mono-layer Graphene Templates, *Adv. Mater. Interfaces*, 2016, **3**(22), 1600621.

4 S. B. Jo, H. H. Kim, H. Lee, B. Kang, S. Lee and M. Sim, *et al.*, Boosting Photon Harvesting in Organic Solar Cells with Highly Oriented Molecular Crystals via Graphene–Organic Heterointerface, *ACS Nano*, 2015, **9**(8), 8206–8219.

5 M. Gobbi, E. Orgiu and P. Samorì, When 2D Materials Meet Molecules: Opportunities and Challenges of Hybrid Organic/Inorganic van der Waals Heterostructures, *Adv. Mater.*, 2018, **30**(18), 14767.

6 M. Halik, H. Klauk, U. Zschieschang, G. Schmid, S. Ponomarenko and S. Kirchmeyer, *et al.*, Relationship Between Molecular Structure and Electrical Performance of Oligothiophene Organic Thin Film Transistors, *Adv. Mater.*, 2003, **15**(11), 917–922, DOI: 10.1002/adma.200304654.

7 M. K. Huss-Hansen, A. E. Lauritzen, O. Bikondoa, M. Torkkeli, L. Tavares and M. Knaapila, *et al.*, Structural stability of naphthyl end-capped oligothiophenes in organic field-effect transistors measured by grazing-incidence X-ray diffraction in operando, *Org. Electron.*, 2017, **49**, 375–381. Available from: http://www.sciencedirect.com/science/article/pii/S1566119 917303440.

8 I. Salzmann, A. Moser, M. Oehzelt, T. Breuer, X. Feng and Z. Y. Juang, *et al.*, Epitaxial growth of π-stacked perfluoropentacene on graphene-coated quartz, *ACS Nano*, 2012, **6**(12), 10874–10883, DOI: 10.1021/nn3042607.

9 H. Peisert, T. Schwieger, J. M. Auerhammer, M. Knupfer, M. S. Golden and J. Fink, *et al.*, Order on disorder: Copper phthalocyanine thin films on technical substrates, *J. Appl. Phys.*, 2001, **90**(1), 466–469, DOI: 10.1063/1.1375017.

10 W. Brütting and C. Adachi, *Physics of Organic Semiconductors*, Wiley, 2nd edn, 2012.

11 H. Huang, Y. Huang, S. Wang, M. Zhu, H. Xie and L. Zhang, *et al.*, van der Waals Heterostructures between Small Organic Molecules and Layered Substrates, *Crystals*, 2016, **6**(9), 113.

12 G. Duva, A. Mann, L. Pithan, P. Beyer, J. Hagenlocher and A. Gerlach, *et al.*, Template-Free Orientation Selection of Rod-Like Molecular Semiconductors in Polycrystalline Films, *J. Phys. Chem. Lett.*, 2019, **10**(5), 1031–1036.

13 S. Kowarik, A. Gerlach and F. Schreiber, Organic molecular beam deposition: Fundamentals, growth dynamics, and in situ studies, *J. Phys.: Condens. Matter*, 2008, **20**(18), 184005.

14 J. J. Cox, S. M. Bayliss and T. S. Jones, Ordered copper phthalocyanine overlayers on InAs and InSb (100) surfaces, *Surf. Sci.*, 1999, **433**, 152–156. Available from: http://www.sciencedirect.com/science/article/pii/S0039602899004860.

15 M. L. M. Rocco, K.-H. Frank, P. Yannoulis and E.-E. Koch, Unoccupied electronic structure of phthalocyanine films, *J. Chem. Phys.*, 1990, **93**(9), 6859–6864, DOI: 10.1063/1.458918.

16 D. Jariwala, T. J. Marks and M. C. Hersam, Mixed-dimensional van der Waals heterostructures, *Nat. Mater.*, 2017, **16**(2), 170–181, DOI: 10.1038/nmat4703.

17 W. Jung, S. J. Ahn, S. Y. Lee, Y. Kim, H.-C. Shin and Y. Moon, *et al.*, Effects of graphene imperfections on the structure of self-assembled pentacene films, *J. Phys. D: Appl. Phys.*, 2015, **48**(39), 395304, DOI: 10.1088/0022-3727/48/39/395304.

18 W. H. Lee, J. Park, S. H. Sim, S. Lim, K. S. Kim and B. H. Hong, *et al.*, Surface-Directed Molecular Assembly of Pentacene on Monolayer Graphene for High-Performance Organic Transistors, *J. Am. Chem. Soc.*, 2011, **133**(12), 4447–4454, DOI: 10.1021/ja1097463.

19 Y. L. Huang, W. Chen, H. Huang, D. C. Qi, S. Chen and X. Y. Gao, *et al.*, Ultrathin films of diindenoperylene on graphite and SiO₂, *J. Phys. Chem. C*, 2009, **113**(21), 9251–9255.

20 M. A. Heinrich, J. Pflaum, A. K. Tripathi, W. Frey, M. L. Steigerwald and T. Siegrist, Enantiotropic Polymorphism in Di-indenoperylene., *J. Phys. Chem. C*, 2007, **111**(51), 18878–18881, DOI: 10.1021/jp0748967.

21 A. K. Tripathi and J. Pflaum, Correlation between ambipolar transport and structural phase transition in diindenoperylene single crystals, *Appl. Phys. Lett.*, 2006, **89**(8), 082103.

22 A. C. Dürr, F. Schreiber, M. Münch, N. Karl, B. Krause and V. Kruppa, *et al.*, High structural order in thin films of the organic semiconductor diindenoperylene, *Appl. Phys. Lett.*, 2002, **81**(12), 2276–2278, DOI: 10.1063/1.1508436.

3102 | *Phys. Chem. Chem. Phys.*, 2020, **22**, 3097–3104

This journal is © the Owner Societies 2020

23 Q. H. Wang, K. Kalantar-Zadeh, A. Kis, J. N. Coleman and M. S. Strano, Electronics and optoelectronics of two-dimensional transition metal dichalcogenides, *Nat. Nanotechnol.*, 2012, **7**, 699, DOI: 10.1038/nnano.2012.193.

24 S. Manzeli, D. Ovchinnikov, D. Pasquier, O. V. Yazyev and A. Kis, 2D transition metal dichalcogenides, *Nat. Rev. Mater.*, 2017, **2**, 17033, DOI: 10.1038/natrevmats.2017.33.

25 M. Xu, T. Liang, M. Shi and H. Chen, Graphene-Like Two-Dimensional Materials, *Chem. Rev.*, 2013, **113**(5), 3766–3798, DOI: 10.1021/cr300263a.

26 K. S. Novoselov, A. Mishchenko, A. Carvalho and A. H. Castro Neto, 2D materials and van der Waals heterostructures, *Science*, 2016, **353**(6298), aac9439. Available from: http://science.sciencemag.org/content/353/6298/aac9439.abstract.

27 L. Britnell, R. M. Ribeiro, A. Eckmann, R. Jalil, B. D. Belle and A. Mishchenko, et al., Strong Light-Matter Interactions in Heterostructures of Atomically Thin Films, *Science*, 2013, **340**(6138), 1311–1314. Available from: http://science.sciencemag.org/content/340/6138/1311.abstract.

28 P. Kumar and B. Viswanath, Horizontally and vertically aligned growth of strained MoS2 layers with dissimilar wetting and catalytic behaviors, *CrystEngComm*, 2017, **19**(34), 5068–5078, DOI: 10.1039/C7CE01162H.

29 R. Ganatra and Q. Zhang, Few-Layer MoS2: A Promising Layered Semiconductor, *ACS Nano*, 2014, **8**(5), 4074–4099, DOI: 10.1021/nn405938z.

30 B. Radisavljevic, A. Radenovic, J. Brivio, V. Giacometti and A. Kis, Single-layer MoS2 transistors, *Nat. Nanotechnol.*, 2011, **6**(3), 147–150. Available from: http://www.ncbi.nlm.nih.gov/pubmed/21278752.

31 M. Chatti, T. Gengenbach, R. King, L. Spiccia and A. N. Simonov, Vertically Aligned Interlayer Expanded MoS2 Nanosheets on a Carbon Support for Hydrogen Evolution Electrocatalysis, *Chem. Mater.*, 2017, **29**(7), 3092–3099, DOI: 10.1021/acs.chemmater.7b00114.

32 C. Liu, D. Kong, P.-C. Hsu, H. Yuan, H.-W. Lee and Y. Liu, et al., Rapid water disinfection using vertically aligned MoS2 nanofilms and visible light, *Nat. Nanotechnol.*, 2016, **11**, 1098, DOI: 10.1038/nnano.2016.138.

33 M. Sojkova, S. Chromik, A. Rosova, E. Dobrocka, P. Hutar and D. Machajdik, et al., MoS2 thin films prepared by sulfurization, *Proc. SPIE*, 2017, **10354**, 103541K.

34 M. Sojková, P. Siffalovic, O. Babchenko, G. Vanko, E. Dobročka and J. Hagara, et al., Carbide-free one-zone sulfurization method grows thin MoS2 layers on polycrystalline CVD diamond, *Sci. Rep.*, 2019, **9**(1), 2001, DOI: 10.1038/s41598-018-38472-9.

35 Y. L. Huang, Y. J. Zheng, Z. Song, D. Chi, A. T. S. Wee and S. Y. Quek, The organic-2D transition metal dichalcogenide heterointerface, *Chem. Soc. Rev.*, 2018, **47**(9), 3241–3264, DOI: 10.1039/C8CS00159F.

36 D. Jariwala, S. L. Howell, K. S. Chen, J. Kang, V. K. Sangwan and S. A. Filippone, et al., Hybrid, Gate-Tunable, van der Waals p–n Heterojunctions from Pentacene and MoS2, *Nano Lett.*, 2016, **16**(1), 497–503.

37 D. Kong, H. Wang, J. J. Cha, M. Pasta, K. J. Koski and J. Yao, et al., Synthesis of MoS2 and MoSe2 Films with Vertically Aligned Layers, *Nano Lett.*, 2013, **13**(3), 1341–1347, DOI: 10.1021/nl400258t.

38 D. W. Breiby, O. Bunk, J. W. Andreasen, H. T. Lemke and M. M. Nielsen, Simulating X-ray diffraction of textured films., *J. Appl. Crystallogr.*, 2008, **41**(2), 262–271, DOI: 10.1107/S0021889808001064.

39 Z. Jiang, GIXSGUI: A MATLAB toolbox for grazing-incidence X-ray scattering data visualization and reduction, and indexing of buried three-dimensional periodic nanostructured films, *J. Appl. Crystallogr.*, 2015, **48**(3), 917–926, DOI: 10.1107/S1600576715004434.

40 N. Mrkyvkova, M. Hodas, J. Hagara, P. Nadazdy, J. Halahovetz and M. Bodik, et al., Diindenoperylene thin-film structure on MoS2 monolayer, *Appl. Phys. Lett.*, 2019, **114**, 251906.

41 A. E. Lauritzen, M. Torkkeli, O. Bikondoa, J. Linnet, L. Tavares and J. Kjelstrup-Hansen, et al., Structural Evaluation of 5,5′-Bis(naphth-2-yl)-2,2′-bithiophene in Organic Field-Effect Transistors with n-Octadecyltrichlorosilane Coated SiO2 Gate Dielectric, *Langmuir*, 2018, **34**(23), 6727–6736, DOI: 10.1021/acs.langmuir.8b00972.

42 M. Sojková, K. Vegso, N. Mrkyvkova, J. Hagara, P. Hutár and A. Rosová, et al., Tuning the orientation of few-layer MoS2 films using one-zone sulfurization, *RSC Adv.*, 2019, **9**, 29645.

43 R. Resel, M. Bainschab, A. Pichler, T. Dingemans, C. Simbrunner and J. Stangl, et al., Multiple scattering in grazing-incidence X-ray diffraction: impact on lattice-constant determination in thin films, *J. Synchrotron Radiat.*, 2016, **23**(pt 3), 729–734. Available from: https://www.ncbi.nlm.nih.gov/pubmed/27140152.

44 V. Holý, U. Pietsch and T. Baumbach, *High-Resolution X-Ray Scattering from Thin Films and Multilayers*, Springer, 1999.

45 B. B. He, *Two-dimensional X-ray Diffraction*, Wiley, 2009.

46 S. Pachmajer, A. O. F. Jones, M. Truger, C. Röthel, I. Salzmann and O. Werzer, et al., Self-Limited Growth in Pentacene Thin Films, *ACS Appl. Mater. Interfaces*, 2017, **9**(13), 11977–11984, DOI: 10.1021/acsami.6b15907.

47 A. C. Mayer, A. Kazimirov and G. G. Malliaras, Dynamics of Bimodal Growth in Pentacene Thin Films, *Phys. Rev. Lett.*, 2006, **97**, 105503.

48 T. Kakudate, N. Yoshimoto and Y. Saito, Polymorphism in pentacene thin films on SiO2 substrate, *Appl. Phys. Lett.*, 2007, **90**, 081903.

49 J. S. Wu and J. C. H. Spence, Electron diffraction of thin-film pentacene, *J. Appl. Crystallogr.*, 2004, **37**, 78–81.

50 W. C. Marra, P. Eisenberger and A. Y. Cho, X-ray total-external-reflection–Bragg diffraction: A structural study of the GaAs-Al interface, *J. Appl. Phys.*, 1979, **50**(11), 6927–6933, DOI: 10.1063/1.325845.

51 M. Hodas, P. Siffalovic, P. Nádaždy, N. Mrkyvková, M. Bodík and Y. Halahovets, et al., Real-Time Monitoring of Growth and Orientational Alignment of Pentacene on Epitaxial Graphene for Organic Electronics, *ACS Appl. Nano Mater.*, 2018, **1**(6), 2819–2826, DOI: 10.1021/acsanm.8b00473.

52 L. Zhang, Y. Yang, H. Huang, L. Lyu, H. Zhang and N. Cao, et al., Thickness-dependent air-exposure-induced phase

This journal is © the Owner Societies 2020

Phys. Chem. Chem. Phys., 2020, **22**, 3097–3104 | **3103**

transition of CuPc ultrathin films to well-ordered one-dimensional nanocrystals on layered substrates, *J. Phys. Chem. C*, 2015, **119**(8), 4217–4223.

53 A. C. Dürr, F. Schreiber, K. A. Ritley, V. Kruppa, J. Krug and H. Dosch, *et al.*, Rapid Roughening in Thin Film Growth of an Organic Semiconductor (Diindenoperylene), *Phys. Rev. Lett.*, 2003, **90**(1), 16104, DOI: 10.1103/PhysRevLett.90.016104.

54 U. Heinemeyer, R. Scholz, L. Gisslén, M. I. Alonso, J. O. Ossó and M. Garriga, *et al.*, Exciton-phonon coupling in diindenoperylene thin films, *Phys. Rev. B: Condens. Matter Mater. Phys.*, 2008, **78**(8), 085210.

55 U. Heinemeyer, K. Broch, A. Hinderhofer, M. Kytka, R. Scholz and A. Gerlach, *et al.*, Real-Time Changes in the Optical Spectrum of Organic Semiconducting Films and Their Thickness Regimes during Growth, *Phys. Rev. Lett.*, 2010, **104**(25), 257401, DOI: 10.1103/PhysRevLett.104.257401.

56 W. R. Salaneck, S. Stafstrom and J. L. Bredas, *Conjugated Polymer Surfaces and Interfaces: Electronic and Chemical Structure of Interfaces for Polymer Light Emitting Devices*, Cambridge University Press, 1996, p. 172.

57 F. C. Spano, Excitons in conjugated oligomer aggregates, films, and crystals, *Annu. Rev. Phys. Chem.*, 2006, **57**(1), 217–243, DOI: 10.1146/annurev.physchem.57.032905.104557.

58 H. Proehl, R. Nitsche, T. Dienel, K. Leo and T. Fritz, In situ differential reflectance spectroscopy of thin crystalline films of PTCDA on different substrates, *Phys. Rev. B: Condens. Matter Mater. Phys.*, 2005, **71**(16), 165207, DOI: 10.1103/PhysRevB.71.165207.

59 H. Proehl, T. Dienel, R. Nitsche and T. Fritz, Formation of Solid-State Excitons in Ultrathin Crystalline Films of PTCDA: From Single Molecules to Molecular Stacks, *Phys. Rev. Lett.*, 2004, **93**, 097403.

60 G. Witte and C. Wöll, Growth of aromatic molecules on solid substrates for applications in organic electronics, *J. Mater. Res.*, 2004, **19**(7), 1889–1916.

61 F. Schreiber, Organic molecular beam deposition: Growth studies beyond the first monolayer, *Phys. Status Solidi A*, 2004, **201**, 1037–1054.

3104 | *Phys. Chem. Chem. Phys.,* 2020, **22**, 3097–3104

This journal is © the Owner Societies 2020